Di- and trioxacyclohexane as structure directing molecules in the synthesis of zeolites omega and ECR-1

Corentin Chatelard, Mathias Dodin, Raquel Martinez-Franco, Alain Tuel

Di- and trioxacyclohexane as structure directing molecules in the synthesis of zeolites omega and ECR-1

Corentin Chatelard1, Mathias Dodin[2], Raquel Martinez-Franco[2], Alain Tuel[1*]

[1]Universit´e de Lyon, Institut de Recherches sur la Catalyse et l'Environnement de Lyon, IRCELYON, UMR CNRS 5256, Université Lyon 1, 2 av. Einstein, 69626 Villeurbanne Cedex, France

[2]IFP Energies Nouvelles-Etablissement de Lyon, Rond-point de l'échangeur de Solaize, BP 3, 69360, Solaize, France

Corresponding author: alain.tuel@ircelyon.univ-lyon1.fr

Keywords: Zeolite omega, ECR-1, synthesis, nuclear magnetic resonance, structure

Abstract

Six-membered ring cyclohexane derivatives with 2 oxygen (1,4-dioxane or *p*-dioxane) and 3 oxygen (1,3,5-trioxane) atoms have been used as organic molecules in the synthesis of zeolites omega (**MAZ** framework type) and ECR-1 (**EON** framework type). Both molecules yield zeolite omega at moderate temperatures with a composition and aluminum distribution similar to those obtained with more standard organics such as the tetramethylammonium cation. If the preparation of zeolite omega with *p*-dioxane was previously known, the use of 1,3,5-trioxane had never been reported in the literature. The most interesting feature of 1,3,5-trioxane is that these molecules could be released from the structure at very low temperature, typically 300°C below the temperature observed with *p*-dioxane. When the alkalinity of synthesis gels was decreased, zeolite omega was progressively replaced by ECR-1 in the presence of 1,3,5-trioxane but not in the presence of *p*-dioxane. The relative proportion of omega and ECR-1 in the different solids has been monitored by X-ray diffraction (XRD) and solid-stare nuclear magnetic resonance (NMR). ^{23}Na NMR of calcined rehydrated solids was found to be particularly adapted to discriminate ECR-1 from zeolites omega in **MAZ**/**EON** mixtures with poorly resolved XRD patterns.

1. Introduction

Zeolites are crystalline microporous inorganic compounds with structures based on an infinitely extending network of corner-sharing TO_4 tetrahedra. Their framework can be regarded as being built of a repetition of “building units” such as the small secondary building units (SBU) or the larger composite building units (CBU) [1]. Zeolite frameworks can also be viewed as a regular stacking of infinite sheets or chains with a unique and distinctive structure. The linkage of these sheets/chains via oxygen atoms frequently results in the formation of pores of molecular dimensions, typically between 0.4 and 0.8 nm diameter. Although these sheets are generally characteristic of a given zeolite structure, they can nonetheless appear in several different frameworks. For example, the structure of zeolite ECR-1 (**EON** framework type) consists of a regular alternation of **MOR** and **MAZ** sheets found in zeolites mordenite and omega (the synthetic analog of natural mazzite), respectively [2,3]. Both mordenite and mazzite are large pore zeolites with a 12 membered ring (12-MR) channel along [001] and a smaller 8-ring (8-MR) along the same direction between 12-ring channels [4-8]. Mazzite possesses an additional 8-ring channel perpendicular to [001] that does not exist in mordenite. According to the stacking sequence between **MOR** and **MAZ** sheets both the 12-ring and the parallel 8-ring channels are preserved in the **EON** structure but their pore openings are significantly smaller than those of mazzite (for example the 12-ring opening in ECR-1 is 0.67 x 0.68 nm while it is 0.74 x 0.74 in mazzite) [3,9]. The structure of mazzite consists of gmelinite cages (*gme*) linked through shared six-ring faces that form columns running parallel to the c-axis. These columns are linked laterally by a 6-fold screw axis to form large 12-MR pores. Many organic molecules have been used to direct the synthesis of zeolite omega from small ammonium cations such as the

tetramethylammonium (TMA^+) cation to bulkier cations or molecules [10-12]. The TMA^+ cation, which appears to be a strong structure directing agent, is small enough to be occluded in the *gme* cages during crystallization [6]. This is not the case of long chain molecules such as hexanediamine or the hexamethonium cation that fill 12-ring channels [13]. Other small molecules such as *p*-dioxane, pyrrolidine or piperazine have also been successfully applied for the crystallization of zeolite omega [14-16]. Although the structure of the different solids was not reported, it is reasonable to assume that some of those molecules were sufficiently small to be located in the *gme* cages, as for TMA^+ cations. With *p*-dioxane, the authors even suggested that the molecule was actually occluded in the form of a dioxane-Na^+ complex that mimics the role of TMA^+ [14]. More recently, zeolite omega was synthesized by hydrothermal conversion of **FAU** and ***BEA**-type zeolites in the absence of organic molecules, using non-calcined seed crystals [17]. Okubo's group also prepared **MAZ**-type zeolites without the help of organic molecules but both the XRD pattern and ^{27}Al NMR spectrum suggested that the solid was rather a **MAZ**/**EON** mixture [18].

ECR-1 was first synthesized in 1987 by Vaughan and Strohmaier using bis-(2-hydroxyethyl)-dimethyl-ammonium cation as structure directing agent [19,20]. Later, the zeolite was obtained in the presence of adamantane-containing diquaternary alkylammonium cations of different chain lengths with Si/Al ratios between 3.7 and 4.4 [21]. More generally, ECR-1 is obtained with Si/Al = 3.5 in the absence of any organic molecule or in the presence of traces of tetramethylammonium cations [3,22]. Gel compositions and crystallization conditions are close to those of mordenite but the latter is rarely found as by-product in the final solid, even when the initial gel in enriched in SiO_2. Despite its structural relationship with mazzite, the synthesis of ECR-1 has never been reported in the presence of 6-ring molecules such as *p*-

dioxane or piperazine. With these molecules, zeolite omega is generally contaminated by mordenite, analcime, gismondine, gmelinite or sodalite [14]. However, the overlap of the XRD pattern of ECR-1 with those of zeolites omega and mordenite makes ECR-1 quite difficult to discriminate from zeolite omega, particularly in mixtures with low ECR-1 contents. The observation of XRD peaks characteristic of the **EON** topology is also often complicated by the broadness and weakness of reflections, resulting from the crystal shape and size and the possible presence of stacking faults between **MAZ** and **MOR** sheets in the framework [3]. Omega/ECR-1 discrimination cannot be made on the basis of ^{29}Si NMR since the spectra of the two zeolites are very similar [3]. In contrast, ^{27}Al NMR spectra of zeolites omega and ECR-1 significantly differ. Both are composed of two signals at ca. 61 and 54 ppm with relative intensities that differ from one zeolite to another [3,23]. In zeolite omega, the two peaks have been assigned to the two crystallographic non-equivalent T1 (ca. 61 ppm) and T2 (ca. 54 ppm) sites of the structure [24]. Since the unit cell contains 24 T1 and 12 T2 sites, the expected theoretical T1/T2 intensity ratio is 2. Experimentally, this ratio is always < 2, suggesting a preferential incorporation of Al species in sites T2, and it typically ranges between 1.4 and 1.8 [23-27]. In ECR-1, the intensity ratio is around 0.5, i.e. the intensity of the line at 54 ppm is approx. twice that of the line at 61 ppm [3]. Although there is no direct relationship between the intensity of ^{27}Al NMR bands in zeolite omega and the framework Al content, T1/T2 ratios smaller than unity could indicate the presence of ECR-1 that was not necessarily detected by XRD.

The present work examines the possibility of synthesizing zeolites omega and ECR-1 using small 6-ring cyclic ether molecules with 2 or 3 oxygen atoms, namely 1,4-dioxane (further named *p*-dioxane) and 1,3,5-trioxane (further named trioxane).

Among them, only *p*-dioxane has been shown to direct the synthesis of zeolite omega but the presence of the **MAZ** sheets and *gme* cavities in both structures suggests that it could also direct the **EON** structure. The influence of various synthesis parameters such as the Na^+ content, the OH^-/SiO_2 and SiO_2/Al_2O_3 ratios in the gel, the crystallization temperature on the formation of both zeolites are discussed. Zeolites are characterized using X-ray Diffraction (XRD), Scanning Electron Microscopy (SEM) Thermogravimetric Analysis (TGA), solid state Nuclear Magnetic Resonance (NMR) and chemical analysis by X-ray fluorescence (FX).

2. Experimental section

2.1. Synthesis of zeolites

Gels were prepared using distilled water, sodium hydroxide (NaOH, Carlo Erba), sodium aluminate ($NaAlO_2$, Riedel de Haen, 54 wt.-% Al_2O_3, 41 wt.-% Na_2O), colloidal silica Ludox® AS-40 (SiO_2, 40 wt. % in water, Sigma-Aldrich) and an organic molecule selected from 1,3,5-trioxane (>99%, Sigma-Aldrich) and 1,4-dioxane (>99%, Alfa Aesar).

In a typical synthesis 0.355 g NaOH and 0.724 g $NaAlO_2$ were dissolved in 5.95 mL of water under stirring. Then 5.58 g Ludox® AS-40 were added dropwise under stirring, followed by 2.53 g trioxane. The gel with the following composition $10SiO_2$ – $0.86Al_2O_3$ – 7.5Trioxane – $2.2Na_2O$ – $142H_2O$ was stirred at room temperature for 3 hours, placed in an autoclave and crystallized at 115°C for 7 days under dynamic conditions (60 rpm). All other syntheses were carried out following the same procedure by changing the amount of NaOH and/or $NaAlO_2$, the temperature and the nature of the organic molecule. After crystallization, solids were recovered by filtration, washed abundantly with distilled water and dried overnight at 80°C.

Eventually, they were further calcined at 550°C in air for 8 hours to remove the organics.

2.2. Characterization

X-ray diffraction (XRD) patterns were recorded at room temperature on a Bruker D8 advance diffractometer (Cu K_α radiation) from 4 to 80° with 0.02° steps and 0.5 s per step.

The amount of organics in the different zeolites was obtained by measuring the weight loss upon heating as-made solids in air in a Mettler Toledo Thermal Analysis apparatus. Samples were heated from 25 to 750°C with a heating rate of 10°C/min.

The overall Si/Al ratio of zeolites was measured by X-ray fluorescence on a Panalytical Epsilon 4 analyzer using a calibration curve previously established on a series of zeolites with well-known compositions.

SEM images were obtained at 2 kV on a Zeiss Supra 40 microscope equipped with an Everhart-Thomley SE2 detector. After dispersion of the zeolite in ethanol, the solution was ultra-sonicated and deposited on an aluminum plot.

All nuclear magnetic resonance (NMR) spectra were recorded on a Bruker Avance III 500 WB spectrometer equipped with a 4mm double-bearing probe head. Samples were spun at 10 kHz in 4 mm zirconia rotors and data were collected at room temperature. ^{1}H-^{13}C CP/MAS spectra were obtained using a standard cross-polarization sequence with a contact time of 1.5 ms and a recycle delay of 5 s. ^{29}Si, ^{27}Al and ^{23}Na MAS spectra were obtained using a “one-pulse” sequence. Pulse lengths and recycle delays were 4 µs (π/3) - 100s, 1µs (π/6) – 1s and 1µs (π/6) -2s for ^{29}Si, ^{27}Al and ^{23}Na, respectively. In the case of ^{23}Na, spectra were recorded on both dehydrated and hydrated solids. For dehydrated solids, rotors were filled with the zeolite and placed at 250°C for 12 h before closing. Spectra were recorded

immediately after closing and the acquisition time was short enough (3 min) to prevent rehydration. Rehydrated zeolites were obtained by contacting powders with a saturated solution of $Mg(NO_3)_2$ for 24 h. ^{29}Si, ^{27}Al and ^{23}Na chemical shifts were referred with respect to tetramethylsilane (TMS), $Al(H_2O)_6^{3+}$ and NaCl, respectively.

3. Results and discussion

3.1. Syntheses with trioxane

The trioxane molecule is known to direct the synthesis of high-silica sodalite in aqueous media [28]. Attempts to use this molecule along with crown ethers to stabilize the *sod* cage and increase the silicon content in **FAU** and **EMT**-type zeolites were unsuccessful [29]. Not only the zeolites obtained did not contain trioxane molecules in *sod* cages but their Si/Al ratio was close to 4 and similar to those obtained in the absence of trioxane. Following a similar approach, syntheses have been performed by crystallizing gels with the composition 10 SiO_2 – 1 Al_2O_3 – 2.2 Na_2O – 0.5 15-crown-5 – x trioxane – 140 H_2O at 115°C for 7 days. As detailed in the experimental section, organic molecules were added after all inorganic compounds in the gel, i.e. according to Method III of Chatelain et al. [29]. For x = 0.5, which corresponds to the gel composition of the literature, **FAU**-type zeolites are only obtained under static conditions. Under stirring, the XRD pattern of the solid is characteristic of zeolite omega contaminated by ECR-1 (Fig. S1). The trioxane/SiO_2 ratio was then increased to 0.75 (x = 7.5), which is the value used by Keijsper et al. to crystallize high-silica sodalite with trioxane in aqueous solutions [28]. After a crystallization period of 7 days, both static and dynamic conditions lead to the formation of pure zeolite omega, the synthetic counterpart of the natural zeolite mazzite (**MAZ** framework topology) (Fig. S2). However, the better resolution and

higher intensity of XRD reflections obtained under stirring made that static conditions were definitely abandoned and that stirring was used as a “standard condition” in all further syntheses.

The ^{13}C NMR spectrum of the as-made zeolite omega consists of a single line at ca. 92.5 ppm characteristic of the trioxane molecule without any signal at 70 ppm corresponding to 15-crown-5, suggesting that the crown ether does not participate in the crystallization of the zeolite framework (Fig. S3). A second experiment performed using the same gel composition but in the absence of 15-crown-5 confirmed that zeolite omega could be effectively obtained without crown ether and that the only templating molecule was trioxane (Fig. 1-a). Moreover, the preparation methods described by Chatelain et al. had no influence on the structure and composition of the final product [29]. Zeolite omega was obtained with Si/Al = 3.26 ± 0.06 whatever the order of addition of the reactants in the gel. The solid appears in the form of bundles of needles of ca. 10 µm long similar to those observed by Vaughan et al. on samples prepared with bis-(2-hydroxyethyl) dimethyl ammonium cations (Fig. 1-b) [20]. Thermogravimetric analysis of the solid shows a nearly continuous weight loss between room temperature and 450°C with an inflection point at 250°C (Fig 2-a). The loss between 25 and 250°C, which corresponds to ca. 10% of the initial mass of solid, can be unambiguously assigned to the removal of water molecules. The second weight loss with a minimum of the DTA curve at 280°C is due to the decomposition of organic molecules. The decomposition temperature is approx. 300°C below that observed on the same material synthesized using TMA^+ cations or *p*-dioxane as organic molecules (Fig. 2-b) [13,14,30]. Such a difference can be explained either by exceptionally weak interactions of the molecule with the zeolite surface or by the chemical nature of trioxane itself and its decomposition products at

high temperature. The first assumption implies that trioxane molecules are not occluded in the *gme* cavities but rather in the 12-MR channel of the framework. Indeed, the thermal stability of organic molecules and their decomposition temperature in air generally increase when the size of the cavity in which they are occluded decreases. This is clearly demonstrated by the difference of 150°C between decomposition temperatures of *p*-dioxane molecules occluded in *sod* and *gme* cages of **SOD** and **MAZ** frameworks, respectively [14]. However, the presence of organic molecules inside the large pores would certainly decrease the amount of internal water molecules and change the T1/T2 ^{27}Al NMR intensity ratio, as already observed in the case of n-hexane derivatives [13]. As it will be discussed in section 3.2, a zeolite prepared using *p*-dioxane as organic molecule under the same experimental conditions showed not only the same framework composition but also similar T1/T2 ratio and water content, making the second assumption more reasonable. Following this assumption, trioxane molecules are effectively located in the *gme* cages but their removal is facilitated by the nature of their decomposition products. Computer simulations have shown that the trioxane molecule perfectly fits the *sod* cage in sodalite whilst *p*-dioxane does not [28]. This was attributed to the replacement of an oxygen atom by a CH_2 group, making *p*-dioxane too bulky for the *sod* cage. Since the [$4^9 6^2 8^3$] gmelinite cavity is smaller than the [$4^6 6^8$] sodalite cage, it would be surprising to observe an opposite behavior in zeolite omega, i.e. that the *gme* cavity can accommodate *p*-dioxane but not trioxane, especially since the 3-fold axis of trioxane is more compatible with the symmetry of the *gme* cavity.

Trioxane molecules in sodalite show an exothermic peak with a maximum at ca. 410°C in the DTA curve corresponding to the decomposition of the molecule into formaldehyde [31]. However, the [$4^9 6^2 8^3$] gmelinite cavity possesses an 8-MR

window that is absent from the [$4^6 6^8$] sodalite cage and that could be large enough to enable the release of formaldehyde from the structure at low temperature. This would be more difficult with *p*-dioxane molecules whose decomposition gives the bulkier acetaldehyde. The location of trioxane in *gme* cavities is also supported by a weight loss between 250 and 450°C that corresponds to approx. 0.85 organic molecules per cavity, a value quite similar to that found in materials prepared with *p*-dioxane [14]. The weight loss is not associated with a thermal effect, thus supporting the decomposition of the molecules into formaldehyde, followed by their direct removal in the gas phase prior to combustion (Fig. 2-a). In contrast, when *p*-dioxane molecules are occluded in *gme* cavities, their removal necessitates a complete burning in air with a strong exothermic peak at ca. 580°C (Fig. 2-b).

3.1.1. Influence of the alkalinity of the gel

The NaOH content in the gel has generally a great influence on the crystallization kinetics of zeolites and their composition [32]. A series of syntheses was performed by decreasing the NaOH content in a gel with the following composition 10 SiO_2 – 0.82 Al_2O_3 – x Na_2O – 7.5 trioxane – 140 H_2O (x varied from 2.5 to 1.7) and the corresponding solids were systematically analyzed by XRD and solid-state NMR. For high alkalinity (Na_2O/SiO_2 = 0.25, x = 2.5) the XRD pattern of the corresponding solid is characteristic of a pure and highly crystalline zeolite omega (Fig. 3-a). No other phase can be detected even at a trace level, thus confirming that trioxane is an excellent structure directing molecule for the **MAZ** topology. When the Na_2O/SiO_2 ratio is decreased to 0.22, XRD reflections significantly broaden and additional peaks appear in the XRD pattern (Fig. 3-b). Those signals have been identified as characteristic of the **EON** topology, suggesting the presence of zeolite ECR-1 in the batch. However, most of XRD reflections of the **EON** topology are also common to

MAZ and **MOR**, which makes ECR-1 difficult to distinguish from a mixture of zeolites omega and mordenite, particularly when reflections are broad [20]. Nonetheless, the presence of a broad signal at 21.2° that exists neither in **MAZ** nor in **MOR** and that can be assigned to the (016) reflection of **EON** definitely supports the presence of ECR-1 rather than a **MOR** + **MAZ** mixture. The XRD pattern is gradually modified when the NaOH content in the initial gel is further decreased (Fig. 3-c to f). Signals at 5.6, 11.1, 16.06 and 16.68° corresponding to the (100), (200), (201) and (300) reflections of **MAZ** decrease with the NaOH concentration and totally disappear for Na_2O/SiO_2 = 0.17 (Fig. 3-f). These observations suggest that zeolite omega is the only product formed at high alkalinity and that it is gradually replaced by ECR-1 when the NaOH content is decreased. In the same time, reflections characteristic of the **MOR** topology such as the (330) reflection at 19.6° were never observed, confirming that mordenite is not formed even at low alkalinities. Structural modifications can also be evidenced by the change in the overall Si/Al ratio of the solids. The ratio continuously increases from 3.8 at Na_2O/SiO_2 = 0.25 to 4.5 at Na_2O/SiO_2 = 0.17 (Table 1). These values agree with those reported in the literature for both zeolites [13,14,26]. Indeed, zeolites omega and ECR-1 generally crystallize with Si/Al ratios between 3 and 5, even though higher values to 9 have been claimed using piperazine as templating molecule [15]. Fig. 4 reports the SEM images of pure zeolites omega and ECR-1 obtained with Na_2O/SiO_2 = 0.25 and 0.17, respectively. Both zeolites possess the same crystal habit but aggregates show very different size and shape. Moreover, **MAZ** crystals are much longer than those of ECR-1 but the difference is not marked enough to distinguish clearly between the two structures in a mixture. The percentage of **MAZ** in the different batches increases with the NaOH concentration and ECR-1 is obtained almost pure at Na_2O/SiO_2 = 0.17. Thermal

analysis data of the different samples show that the decomposition temperature of trioxane does not change from zeolite omega to ECR-1, suggesting that molecules are in similar environments in both structures, most likely in *gme* cavities (Fig. S4). When omega is replaced by ECR-1, the relative amount of organic matter decreases, which is a direct consequence of their respective unit cell compositions. However, the percentage of *gme* cavities occupied by trioxane molecules does not significantly change and corresponds to approx. 85% for both zeolites omega and ECR-1.

The composition of the different batches can be estimated by looking at the evolution of some of the reflections characteristic of **MAZ** and **EON** structures in the XRD patterns. This could be done without using an internal standard by considering that the total intensity of the pattern I_{tot} is the sum of the intensities I_{MAZ} and I_{EON} corresponding to **MAZ** and **EON** structures, weighted by their respective fractions in the mixture: $I_{tot} = xI_{MAZ} + (1-x)I_{EON}$, where $0 < x < 1$. Assuming that the solid obtained at $Na_2O/SiO_2 = 0.25$ ($x = 1$) is a pure zeolite omega, the evolution of (201) and (300) lines characteristic of the **MAZ** topology at 16.1 and 16.7°, respectively, leads to the different compositions reported in Table 1. Even though the percentages obtained for $Na_2O/SiO_2 < 1.9$ cannot be precisely estimated because of low intensity of XRD reflections, values in Table 1 clearly show how the formation of ECR-1 is sensitive to the NaOH concentration in the gel. An additional synthesis was performed using a NaOH content corresponding to $Na_2O/SiO_2 = 0.18$ but NaCl was added in the gel so that the overall $Na_2O/SiO_2 = 0.25$. The corresponding XRD pattern (not shown) and Si/Al ratio (Table 1) were similar to those obtained in the absence of NaCl, thus confirming that the critical parameter in the formation of ECR-1 is not the Na content but the pH value.

The series of solids obtained at various Na_2O/SiO_2 ratios was also characterized by ^{29}Si and ^{27}Al MAS NMR. Zeolites omega and ECR-1 obtained with Na_2O/SiO_2 ratios of 0.25 and 0.17, respectively, show very similar ^{29}Si NMR spectra with 5 signals between -115 and -85 ppm attributed to Si(nAl) atoms, n comprised between 0 and 4 being the number of Al atoms in the first coordination sphere of Si (Fig. S5). Relative intensities slightly differ probably because of different Al contents in the frameworks (Table 1). In zeolite omega, the decomposition of ^{29}Si NMR spectra is difficult due to the overlap of two sets of signals corresponding to T1 and T2 sites respectively and the calculation of the Si/Al ratio from line intensities is not straightforward [24-26,33]. The differentiation between **MAZ** and **EON** topologies is thus almost impossible on the basis of ^{29}Si MAS NMR alone, particularly for mixtures in which the two zeolites are present. In contrast, ^{27}Al NMR spectra change a lot with the percentage of zeolite omega in the solid (Fig. 5). The **MAZ** structure contains two non-equivalent crystallographic sites T1 and T2 with relative multiplicities of 2:1. T1 is located in the 4-membered rings of *gme* cages while T2 occupies the 6-membered rings that link these cages together. As a consequence the two signals at ca. 61 and 54 ppm in the ^{27}Al NMR spectrum of zeolite omega have been attributed to Al atoms in T1 and T2, respectively [24]. In most of zeolites omega, the ratio I_{61}/I_{54} between the intensities of the two NMR peaks is smaller than 2, suggesting that Al is not randomly distributed in the framework but preferentially located in site 2, i.e. in the 6-rings between *gme* cages [25-27]. This ratio does not necessarily depend on the Al content but rather on synthesis conditions. In fact, zeolites with the same Al content can have very different I_{61}/I_{54} ratios whereas similar ratios have been observed on solids with various compositions [26]. Omega zeolites recovered at different crystallization times even showed that the preferential incorporation of Al species into

six-membered rings decreases with crystal growth, giving rise to a spatial Al-zoning [34]. Additionally, it has been reported that the ratio could not be correctly determined by deconvolution of the 1-dimensional NMR spectrum with Gaussian or Lorentzian lines, particularly when spectra are recorded at low magnetic fields. Indeed, ^{27}Al being a quadrupolar nuclei (S = 5/2) lines are not symmetrical and their width and overlap vary with the magnetic field of the spectrometer. Wouters et al. have shown that a better determination of the I_{61}/I_{54} ratio could be made using the real line shape for the two signals obtained from 2D-3Q MAS NMR spectra [23]. For a zeolite with an overall Si/Al ratio of 3.67, deconvolution of a spectrum recorded in a magnetic field of 9.4 T (^{1}H frequency 400 MHz) gave I_{61}/I_{54} = 1.75 using the real line shapes but only 0.87 using Lorentzian line shapes. The difference is certainly less pronounced for spectra in Fig. 5 since they have been recorded in a high magnetic field of 11.7 T (500 MHz). Therefore, spectra were deconvoluted using two lines with constant width and shape (a combination of Lorentzian and Gaussian lines), i.e. only the position and intensity of the lines were changed throughout the series (Fig. 5, inset). At Na_2O/SiO_2 = 0.25, a pure zeolite omega is characterized by I_{61}/I_{54} = 0.95, in agreement with previous T1/T2 ratios obtained experimentally by deconvoluting NMR spectra with Lorentzian lines (Table 1) [26]. The spectrum of the zeolite obtained at Na_2O/SiO_2 = 0.17 shows an I_{61}/I_{54} ratio of 0.32 and looks very similar to the ^{27}Al NMR spectrum of ECR-1 reported in the literature (Table 1) [3]. Assuming that the Si/Al ratio and the distribution of Al species on T1 and T2 sites in zeolite omega (Si/Al = 3.8 and I_{61}/I_{54} = 0.95) do not change with the percentage of ECR-1 in the mixture, the evolution of NMR signals at 54 and 61 ppm with the NaOH content in Fig. 5 is a direct consequence of the presence of ECR-1. By contrast to zeolite omega, ^{27}Al NMR signals of ECR-1 have not been assigned to the different crystallographic sites

of the structure. Nevertheless, assuming that sites in **MAZ** sheets of the **EON** structure have the same chemical shifts as in zeolite omega, the signal at 61 ppm can be attributed to T1, T2 and T3 whilst that at 54 ppm corresponds to sites T4 to T10 of the **EON** framework (ESI). Taking into account the multiplicity of all sites in the unit cell and considering a homogeneous distribution of Al in the framework, a "theoretical" intensity ratio I_{61}/I_{54} = 0.66 is obtained. This value is certainly approximate since a recent work has reported an inhomogeneous distribution of Al in the **EON** framework with Al-rich **MAZ** and Al-poor **MOR** sheets [35].

Even if I_{61}/I_{54} values are not precisely determined, the evolution of the ratio within the series can be used to evaluate the percentages of **MAZ** and **EON** zeolites in the solid (ESI). Values listed in Table 1 are in good agreement with those obtained by XRD.

3.1.2. Influence of the Al content in the gel

All above syntheses were performed with SiO_2/Al_2O_3 = 10 in the gel, which was the value used to prepare omega zeolites with *p*-dioxane in the literature [14]. Changing the Al content in the gel may have an influence on the composition of the framework but also on the nature of the zeolites formed. A series of syntheses has been performed using the same gel composition except that the amount of sodium aluminate was changed (Table 2). For each composition, the mass of NaOH was recalculated in order to keep the pH value constant as well as the Na_2O/SiO_2 ratio at 0.22. Low Al contents (SiO_2/Al_2O_3 = 60) favor the formation of sodalite with Si/Al = 13.5, as already reported by Keijsper et al. who obtained sodalite under quite similar conditions with SiO_2/Al_2O_3 = 57 in the gel [28]. Increasing the Al content to SiO_2/Al_2O_3 = 20 produces mordenite with a framework Si/Al ratio of 4.64, slightly higher than ratios obtained on the **MAZ**-**EON** series. Under the present conditions, mordenite

crystallizes in the absence of organic molecules, as evidenced by ATG. At higher Al contents (SiO_2/Al_2O_3 = 14), the XRD pattern of the solid formed is characteristic of a **MAZ**/**EON** mixture, similar to those obtained previously with SiO_2/Al_2O_3 = 10 and low Na_2O/SiO_2 ratios. The solid is characterized by Si/Al = 4.25 and an intensity ratio measured on the ^{27}Al NMR spectrum I_{61}/I_{54} = 0.43 (Table 2). Comparison with data in Table 1 obtained on solids prepared with various NaOH concentrations indicates that the solid contains approx. 70 wt.-% ECR-1. For SiO_2/Al_2O_3 ratios between 10 and 12, zeolite omega is the only zeolite formed. The framework Si/Al ratio of the zeolite depends on the Al content in the gel and increases from 3.3 at SiO_2/Al_2O_3 = 10 to 4.0 at SiO_2/Al_2O_3 = 12 (Table 2). Finally, high Al concentrations in the gel (SiO_2/Al_2O_3 = 6) lead to a mixture of sodalite and zeolite P. The **MAZ** topology is thus formed within a very narrow range of Al_2O_3/SiO_2 ratios (typically between 10 and 15) and can be easily contaminated by zeolite ECR-1. The relative proportion of **MAZ** in the **MAZ**/**EON** mixture is very sensitive to the Al content in the gel.

3.1.3. Influence of the trioxane concentration

Most of above syntheses were performed with an excess of trioxane in the gel. The **MAZ** structure contains two *gme* cages per unit cell. Assuming that all cages are filled with one trioxane molecule, the trioxane/(Si+Al) ratio in the solid is 2/36 = 0.056. For 12 T atoms (T = Si or Al) in the gel, this corresponds to 0.66 trioxane molecule. Additional syntheses performed with 4, 2 and 1 trioxane molecules/10SiO_2 in the gel (keeping Na_2O/SiO_2 = 0.22 and SiO_2/Al_2O_3 = 10) also produced zeolite omega at 115°C, thus confirming the minor influence of the organic content on the crystallization (Fig. S6). Solids obtained with 7.5, 4 or 2 trioxane molecules/10SiO_2 possess approx. the same framework Al content (Si/Al = 3.25 ± 0.05) but this ratio increases to 3.85 when the trioxane content is decreased to 1 molecule/10SiO_2. In

the same time, the XRD pattern significantly broadens and additional weak signals suggest the presence of ECR-1. The presence of ECR-1 at low trioxane concentration confirms our observations on syntheses performed with trioxane/15-crown-5 mixtures at trioxane/SiO_2 = 0.05.

3.1.4. Influence of the crystallization temperature.

Zeolite omega is generally obtained at moderate temperatures, typically between 100 and 150°C. The crystallization temperature depends on the nature of the templating molecule and increases from 100-110°C with the TMA^+ cation to 150°C with *p*-dioxane or piperazine [10,12,14,16]. When the crystallization temperature of gels with the composition 10 SiO_2 – 1 Al_2O_3 – 2.2 Na_2O – 7.5 trioxane – 140 H_2O is increased from 115 to 130 °C the nature and crystallinity of the obtained zeolites do not change (Fig. S7). All products are pure zeolites omega as evidenced by x-ray diffraction and their composition is the same within experimental error (Si/Al = 3.2 ± 0.05). At 140°C, zeolite omega is still the major component of the solid but new peaks in the XRD pattern reveal the presence of sodalite (Fig. S7). By contrast, when crystallizations are performed with Na_2O/SiO_2 = 0.17, increasing the temperature from 115 to 130°C significantly improves the crystallinity of ECR-1. The solid is pure and highly crystalline, with a XRD pattern similar to that obtained on solids prepared in the literature with TMA^+ cations (Fig. 6-a) [3]. Compared to a solid crystallized at 115°C, ECR-1 is characterized by I_{61}/I_{54} = 0.32 and Si/Al = 4.49, indicating that temperature has only little influence on the composition and on the distribution of Al species in the framework (Table 1). Apart from the crystallinity, temperature has also a strong effect on the crystal size of the zeolite, as can be seen by comparing SEM images in Figs 4-b, c and 6-b, c. At 130°C, a decrease of the trioxane/SiO_2 from 0.75 to 0.5 leads to the formation of mordenite as by-product; which was not observed at

lower temperature (Fig. S8). Since mordenite was not observed in syntheses performed at 130°C with Na_2O/SiO_2 = 0.22 or at 115°C with Na_2O/SiO_2 = 0.17, the formation of this zeolite has to be attributed to a combination of high temperature and low alkalinity.

3.2 Syntheses with 1,4-dioxane

The 1,4-dioxane (or *p*-dioxane) molecule has been previously reported to direct the crystallization of zeolite omega under static conditions at 140-150°C using Na_2O/SiO_2 ratios in the range 0.2-0.25 [14]. Depending on the dioxane content and the Na_2O/SiO_2 ratio in the gel, solids with Si/Al ratios between 3.2 and 4.1 could be obtained. Other zeolites such as sodalite (**SOD**), gmelinite (**GME**), gismondine (**GIS**), mordenite (**MOR**) and eventually analcime (**ANA**) were also observed but the presence of ECR-1 (**EON**) was never mentioned [14]. In order to compare the templating role of di and trioxane molecules, a synthesis was first performed with *p*-dioxane under the same conditions as those used for trioxane. A gel with the composition 10 SiO_2 – 1 Al_2O_3 – 2.2 Na_2O – 7.5 *p*-dioxane – 140 H_2O was crystallized at 115°C for 7 days under stirring conditions. The solid obtained is a pure and highly crystalline zeolite omega with a framework Si/Al ratio of 3.37, very similar to that obtained with trioxane (Si/Al = 3.31) (Fig. 7-a). The I_{61}/I_{54} ratio measured by ^{27}Al NMR (0.87) is the same as that measured on a sample prepared with trioxane (0.88) under similar conditions. The crystals possess the usual needle-like habit but their size is drastically smaller than with trioxane (Fig. 7-b, c).

Syntheses performed with trioxane have shown that one of the main parameters that governs the formation of ECR-1 is the pH value of the gel. Two gels with the composition 10 SiO_2 – 0.82 Al_2O_3 – x Na_2O – 7.5 p-dioxane – 140 H_2O with x = 2.2 and 1.7 were crystalized for 7 days at 115°C. With trioxane, the same gel

composition gave pure **MAZ** for x = 2.2 and **EON** at x = 1.7, with **MAZ**/**EON** mixtures at intermediates values (Fig. 3). For both Na_2O concentrations the XRD pattern of the corresponding solid is characteristic of the **MAZ** topology but reflections become slightly broader and significantly less intense at low Na_2O/SiO_2 ratio (Fig. 8-a, b). In the absence of additional reflections, these changes have been attributed to a lower crystallinity of the zeolite rather than to the presence of ECR-1. In the same time, the Si/Al ratio of the zeolite increases from 3.83 at x = 2.2 to 4.38 at x = 1.7. These ratios are very similar to those obtained with trioxane, which suggests that the influence of the organic molecule on the incorporation of Si and Al species in the framework is negligible (Table 1).

Previous syntheses with trioxane have shown that the crystallization temperature could greatly affect the crystallinity of ECR-1 obtained at low pH value. An experiment performed at 130°C with x = 1.7 did not significantly improve the crystallinity of the solid (Fig. 8-c). The XRD pattern is quite similar to that of the zeolite obtained with trioxane at 115°C with the same Na_2O/SiO_2 ratio (Fig. 3), and both the high Si/Al value (Si/Al = 4.83) and low I_{61}/I_{54} ^{27}Al NMR intensity ratio (I_{61}/I_{54} = 0.45) suggest the presence of ECR-1 (Fig. S9). However, in the absence of noticeable signal at 21.2° in the XRD pattern, the presence of ECR-1 in the solid cannot be unambiguously demonstrated. Indeed, a simple mixture of zeolites with **MAZ** and **MOR** topologies (90 wt.-% **MAZ** + 10 wt.-% **MOR**) gives a similar XRD pattern with comparable Si/Al and I_{61}/I_{54} ratios (Fig. S10). Nevertheless, the absence of signal at 21.2° does not necessarily mean that ECR-1 is totally absent from the solid but that it is simply not detected by XRD. This could be due either to a small amount of ECR-1 with respect to other zeolites or to quite broad reflections resulting from very tiny crystals. Attempts to increase a hypothetical fraction of ECR-1 in the

final solid were unsuccessful. Increasing the amount of Al in the gel (SiO_2/Al_2O_3 = 10) favored the formation of the **MAZ** topology whilst mordenite was the main zeolite formed when syntheses were carried out at 140°C.

Since the discrimination between ECR-1 and mixtures of zeolites omega and mordenite by XRD is difficult when reflections are broad, samples have been calcined and characterized by ^{23}Na MAS NMR spectroscopy. There are two different positions for Na^+ cations in the **MAZ** structure, each one balancing the charge of Al atoms located in sites T1 and T2 [13]. In ECR-1, sodium is distributed over five different extraframework sites, Na1, Na3 and Na3b being located in the 12-MR channel, Na2 in the 8-MR channel of the **MAZ** sheet and Na4 in the 8-ring channel of the **MOR** sheet [3]. The ^{23}Na MAS NMR spectrum of calcined ECR-1 shows a broad signal with a maximum at ca. -20 ppm, both in the dehydrated and rehydrated forms (Fig. 9). The different crystallographic positions are not resolved, contrasting with the partially resolved ^{27}Al NMR spectrum [3]. A similar broad signal is observed on calcined rehydrated mordenite with a maximum at ca. -16 ppm (not shown). On the contrary the spectrum of a calcined rehydrated zeolite omega is composed of two distinct and well-separated signals with maxima at ca. -9 and -25 ppm (Fig. 9). These peaks can be unambiguously attributed to the 2 extraframework positions for Na^+ cations in the **MAZ** structure. ^{23}Na is a spin 3/2 nucleus and is therefore quadrupolar, with line shapes that depend on the local environment around the cation. Though not symmetrical, a rapid deconvolution of the spectrum with using a combination of Lorentzian and Gaussian lines gives a I_{-25}/I_{-9} ratio close to 2, suggesting that lines at -25 and -9 ppm correspond to Na1 and Na2 sites, respectively. The difference between ^{23}Na NMR signals of **MAZ** and **EON** topologies can be used as an additional tool to discriminate between the two structures. In the case of solids

prepared with trioxane and various Na_2O/SiO_2 ratios, the evolution of ^{23}Na NMR spectra supports the change of structure from **EON** to **MAZ** when the Na_2O/SiO_2 ratio increases from 0.18 to 0.25 (Fig. 10). Assuming that intermediate spectra can be decomposed using those corresponding to pure zeolites omega and ECR-1 (Fig. 10, inset), the fraction of each zeolite can be estimated in the different solids (Table 1). Though less accurate than those obtained by ^{27}Al NMR, the percentages of **MAZ** and **EON** follow the same trend and are also comparable with those estimated from XRD patterns.

^{23}Na NMR was then used to characterize the zeolite obtained at 130°C with Na_2O/SiO_2 = 1.7 and *p*-dioxane as organic template, for which the presence of ECR-1 was questionable (Fig. 8-c). The ^{23}Na NMR spectrum is complex and does not correspond to the spectrum of ECR-1, as it was the case with trioxane. It clearly shows signals characteristic of zeolite omega along with a broad line with a chemical shift intermediate between those of ECR-1 and mordenite (Fig. S11). The spectrum could not be fitted using **MAZ** and E**ON** signals only but the fit was greatly improved when a third component corresponding to **MOR** was added. The best fit corresponds to approx. 44% **MAZ**, 44% **EON** and 12% **MOR**. The relatively small fraction of ECR-1 in the solid may explain why the (016) reflection of the **EON** topology was hardly detectable at 21.2° on the corresponding XRD pattern (Fig. 8-c). In contrast with trioxane, all zeolites prepared using *p*-dioxane at relatively low alkalinity showed similar ^{23}Na NMR spectra with a significant proportion of zeolite omega, indicating that *p*-dioxane is not a good structure directing molecule for the **EON** topology.

4. Conclusion

The 1,3,5-trioxane molecule has demonstrated a strong ability to direct the crystallization of zeolites omega and ECR-1 under mild hydrothermal conditions. Even though the location of organic molecules in the structure could not be determined, it is reasonable to assume that trioxane molecules are occluded in the *gme* cavities present in the two materials, likely as a [Na^+-trioxane] complex. Zeolite omega, which is obtained from highly alkaline gels, is progressively replaced by ECR-1 when the OH^-/SiO_2 ratio is decreased. Zeolites omega and ECR-1 possess the same morphology, typically bundles of elongated needle-like crystals, but the size of individual crystals significantly decreases from omega to ECR-1. The change in product selectivity has been monitored and quantified by XRD, ^{27}Al and ^{23}Na solid state NMR, all three techniques enabling an estimation of the percentage of each zeolite in the solid. Both omega and ECR-1 zeolite are obtained with Si/Al ratios between 3 and 5, which is the value commonly obtained with more standard organic molecules such as the tetramethylammonium cation. Similarly, zeolite omega is obtained with *p*-dioxane under very close conditions but decreasing the alkalinity of the gel does not lead to pure ECR-1, as observed with 1,3,5-trioxane. The nature of the solid is very sensitive to the composition of the gel and mordenite is often observed as a co-crystallized product, suggesting that *p*-dioxane is a less effective structure directing agent for the **EON** topology. Moreover, the decomposition temperature of *p*-dioxane molecules in air is approx. 300°C higher than that observed with trioxane, which makes trioxane particularly interesting for large scale production of zeolite omega.

CRediT authorship contribution statement

Corentin Chatelard: Conceptualization, Methodology, Experiments, Validation, Investigation. **Mathias Dodin**: Conceptualization, Supervision, Project administration, Funding acquisition, Writing – Review and Editing. **Raquel Martinez-Franco**: Conceptualization, Supervision, Project administration, Funding acquisition, Writing – Review and Editing. **Alain Tuel**: Conceptualization, Validation, Writing - Original draft, Writing – Review and Editing, Visualization, Supervision.

Declaration of competing interest

The authors declare that they have no known competing financial interest or personal relationships that could have appeared to influence the work reported in this paper.

Acknowledgments

This work was financially supported by IFPEN within the framework of a PhD grant (Corentin Chatelard).

Appendix A. Supplementary data

Supplementary data related to this work can be found at …

References

1) L.B. McCusker, F. Liebau, G. Engelhardt, Nomenclature of structural and compositional characteristics of ordered microporous and mesoporous materials

with inorganic hosts (IUPAC recommendations 2001), Microporous and Mesoporous Mater. 58 (2003) 3-13, https://doi.org/10.1016/S1387-1811(02)00545-0

2) M.E. Leonowicz, D.W.E. Vaughan, Proposed synthetic zeolite ECR-1 structure gives a new zeolite framework topology, Nature, 329 (1987) 819-821, https://doi.org/10.1038/329819a0

3) A.F. Gualtieri, S. Ferrari, E. Galli, F. Di Renzo, W. van Beek, Rietveld structure refinement of zeolite ECR-1, Chem. Mater. 18 (2006) 76-84, https://doi.org/10.1021/cm051985s

4) W.M. Meier, The crystal structure of mordenite (ptilolite), Z. Kristallogr. 115 (1961) 439-450, https://doi.org/10.1524/zkri.1961.115.5-6.439

5) A. Alberti, P. Davoli, G. Vezzalini, The crystal structure refinement of a natural mordenite, Z. Kristallogr. 175 (1986) 249-256, https://doi.org/10.1524/zkri.1986.175.3-4.249

6) A. Martucci, A. Alberti, M.D. Guzman-Castillo, F. Di Renzo, F. Fajula, Crystal structure of zeolite omega, the synthetic counterpart of the natural zeolite mazzite, Microporous Mesoporous Mater. 63 (2003) 33-42, https://doi.org/10.1016/S1387-1811(03)00429-3

7) E. Galli, E. Passaglia, and D. Pongiluppi, Mazzite, a new mineral, the natural counterpart of the synthetic zeolite Omega, Contr. Mineral. Petrol. 45, (1974) 99-105, https://doi.org/10.1007/BF00371162

8) R. Arletti, E. Galli, G. Vezzalini, W.S. Wise, Mazzite-Na, a new zeolite from Boron, California: Its description and crystal structure, American Mineralogist 90 (2005) 1186-1191, https://doi.org/10.2138/am.2005.1771

9) Database of zeolite structures, http://www.iza-structure.org/databases/

10) A.J. Perrotta, C. Kibby, B.R. Mitchell, E.R. Tucci, Synthesis, characterization and catalytic activity of omega and ZSM-4 zeolites, J. Catal. 55 (1978) 240-249, https://doi.org/10.1016/0021-9517(78)90210-5

11) A. Araya, T.J. Barber, B.M. Lowe, D.M. Sinclair, A. Varma, The synthesis and thermal behavior of zeolite omega, Zeolites 4 (1984) 263-269, https://doi.org/10.1016/0144-2449(84)90036-8

12) F. Fajula, M. Verapacheco, F. Figueras, Synthesis of zeolite omega – Influence of the temperature and the reagents on the crystallization kinetics, Zeolites 7(1987) 203-208, https://doi.org/10.1016/0144-2449(87)90051-0

13) A.M. Goossens, E.J.P. Feijen, G. Verhoeven, B.H. Wouters, P.J. Grobet, P.A. Jacobs, J.A. Martens, Crystallization of MAZ-type zeolites using tetramethylammonium, sodium and n-hexane derivatives as structure- and composition-directing agents, Microporous Mesoporous Mater. 35-36 (2000) 555-572, https://doi.org/10.1016/S1387-1811(99)00250-4

14) B. De Witte, J. Patarin, J.L. Guth, T. Cholley, Synthesis of mazzite-type zeolites in the presence of organic solvents: study of the structure directing role of *p*-dioxane, Microporous Mater. 10 (1997) 247-257, https://doi.org/10.1016/S0927-6513(97)00013-8

15) H. Xu, P. Dong, L. Liu, J.-G. Wang, F. Deng, J.-X. Dong, Synthesis and characterization of zeolite mazzite analogue in Na_2O–Al_2O_3–SiO_2–Piperazine–H_2O, J Porous Mater 17 (2007) 97–101, https://doi.org/10.1007/s10934-006-9013-2

16) M.K. Rubin, C.J. Plank, E.J. Rosinski, Synthesis of zeolite ZSM-4, U S Patent 4,021,447(1977)

17) K. Honda, A. Yashiki, M. Sadakane, T. Sano, Hydrothermal conversion of FAU and *BEA-type zeolites into MAZ-type zeolites in the presence of non-calcined seed crystals, Microporous Mesoporous Mater. 196 (2014) 254-260, http://dx.doi.org/10.1016/j.micromeso.2014.05.028

18) A. Ogawa, K. Iyoki, Y. Kamimura, S.P. Elangovan, K. Itabashi, T. Okubo, Seed-directed, rapid synthesis of MAZ-type zeolites without using organic structure-directing agent, Microporous Mesoporous Mater. 186 (2014) 21-28, http://dx.doi.org/10.1016/j.micromeso.2013.11.026

19) D.E.W. Vaughan, K.J. Strohmaier, Crystalline zeolite (ECR-1) and process for preparing it, US Pat. 4,657,748 (1987)

20) D.E.W. Vaughan, K.J. Strohmaier, Synthesis of the new large-pore zeolite ECR-1, in Zeolite Synthesis, M.L. Occelli, H.E. Robson, Eds, ACS Symp. Ser. 398 (1989) pp 506-517, American Chemical Society, Washington DC.

21) C.S.H. Chen, J.L. Schlenker, S.E. Wentzek, Synthesis and characterization of synthetic zeolite ECR-1, Zeolites 17 (1987) 393-400, https://doi.org/10.1016/0144-2449(96)00039-5

22) J. Song, L. Dai, Y. Ji, F.-S. Xiao, Organic Template Free Synthesis of Aluminosilicate Zeolite ECR-1, Chem. Mater. 18 (2006) 2775-2777, https://doi.org/10.1021/cm052593o

23) B.H. Wouters, T. Chen, A.M. Goossens, J.A. Martens, P.J. Grobet, Determination of the Al^{T1}/Al^{T2} Ratio in MAZ Zeolites Using Line Shapes of MQ MAS NMR, J. Phys. Chem. B 103 (1999) 8093-8096, https://doi.org/10.1021/jp991722j

24) J. Klinowski, M.W. Anderson, J.M Thomas, On the siting of aluminum in zeolite omega, Chem. Commun. 9 (1983) 525-526, https://doi.org/10.1039/c39830000525

25) C.A. Fyfe, G.C. Gobbi, G.J. Kennedy, J.D. Graham, R.S. Ozubko, W.J. Murphy, A. Bothner-By, J. Dadok, A.S. Chesnick, Detailed interpretation of the ^{29}Si and ^{27}Al high-field MAS NMR spectra of zeolites offretite and omega, Zeolites 5 (1985) 179-183, https://doi.org/10.1016/0144-2449(85)90027-2

26) P. Massiani, F. Fajula, F. Figueras, J. Sanz, ^{29}Si and ^{27}Al MAS NMR study of the distribution of Si and Al atoms in various forms of synthetic zeolite omega, Zeolites 8 (1988) 332-337, https://doi.org/10.1016/S0144-2449(88)80132-5

27) J. Klinowski, M.W. Anderson, A High-resolution solid-state nuclear magnetic resonance study of the ordering of silicon and aluminium in synthetic mazzite (zeolite omega), J. Chem. Soc. Faraday Trans. I 82 (1986) 569-584, https://doi.org/10.1039/f19868200569

28) J. Keijsper, C.J.J. den Ouden, M.F.M. Post, Synthesis of high silica sodalite from aqueous systems - a combined experimental and model based approach, in Zeolites: Facts. Figures. Future, P. A. Jacobs. R. A. van Santen Eds., Stud. Surf. Sci. Catal. Vol 49A, pp. 237 247. Elsevier Publishing Company, Amsterdam 1989.

29) T. Chatelain, J. Patarin, M. Soulard, J.L. Guth, P. Schulz, Synthesis and characterization of high-silica EMT and FAU zeolites prepared in the presence of crown-ethers with either ethylene glycol or 1,3,5-trioxane, Zeolites 15 (1995) 90-96, https://doi.org/10.1016/0144-2449(94)00021-J

30) F. Zhang, L. Zhang, Z. Yang, S. Han, Q. Zhu, L. Wang, C. Liu, X. Meng, F.-S. Xiao, Design of fast crystallization of nanosized zeolite omega crystals at higher temperatures, Chin. J. Catal. 40 (2019) 1093-1099, https://doi.org/10.1016/S1872-2067(19)63280-8

31) L. Leardini, A. Martucci, G. Cruciani, The unusual thermal expansion of pure silica sodalite probed by in situ time-resolved synchrotron powder diffraction, Microporous Mesoporous Mater. 151 (2012) 163-171, https://doi.org/10.1016/j.micromeso.2011.10.042

32) M.L. Guzman Castillo, F. Di Renzo, F. Fajula, J. Bousquet, Crystallization kinetics of zeolite omega, the synthetic analog of mazzite, Microporous and mesoporous Mater. 90 (2006) 221-228, https://doi.org/10.1016/j.micromeso.2005.10.022

33) R.H. Jarman, A.J. Jacobson, M.T. Melchior, Interpretation of the Si-29 nuclear magnetic resonance spectra of zeolites – synthetic mazzite, J. Phys. Chem 88 (1984) 5748-5752, https://doi.org/10.1021/j150667a057

34) P. Massiani, F. Fajula, F. Di Renzo, Zoning of Aluminium among Different Crystallographic Sites in Zeolite Omega, Chem. Commun. 12 (1988) 814-815, https://doi.org/10.1039/c39880000814

35) J.H. Shin, N.H. Ahn, S.J. Cho, L.M. Ren, F.S. Xiao, S.B. Hong, Framework Al zoning in zeolite ECR-1, Chem. Commun 50 (2014) 1956-1958, https://doi.org/10.1039/c3cc48403c

Table 1 Influence of the alkalinity on the Si/Al ratios and percentages of **MAZ** in solids obtained from the crystallization of gels with the composition: 10 SiO_2 – 0.82 Al_2O_3 – x Na_2O – 7.5 trioxane – 140 H_2O at 115°C for 7 days.

x	Si/Al	I_{61}/I_{54} ratio	MAZ (%) in the solid		
			XRD	^{27}Al NMR	^{23}Na NMR
2.5	3.79	0.95	100	100	100
2.2	4.04	0.83	80	85	75
2.0	4.21	0.69	50	55	50
1.9	4.36	0.56	35	40	40
1.8	4.47	0.37	20	20	25
1.7	4.48	0.31	0	0	0
2.5[a]	3.81	0.92	97	100	100

[a]The amount of sodium corresponds to 3.6 NaOH + 1.4 NaCl

Table 2 Influence of the SiO_2/Al_2O_3 on the nature and composition of zeolites obtained from the crystallization of gels with the composition: 10 SiO_2 – x Al_2O_3 – 2.2 Na_2O – 7.5 trioxane – 140 H_2O at 115°C for 7 days

x	0.167	0.5	0.714	0.833-1	1.667
SiO_2/Al_2O_3	60	20	14	10-12	6
Zeolite	SOD	MOR	MAZ+EON	MAZ	SOD+GIS
Si/Al ratio	13.5	4.64	4.25	3.3-4.0	n.d.

Figure captions

Fig. 1 XRD pattern (a) and SEM pictures (b) of zeolite omega obtained from the crystallization of a gel with the composition $10SiO_2$ – $1Al_2O_3$ – $2.2Na_2O$ – 7.5 trioxane – 140 H_2O at 115°C for 7 days under dynamic conditions.

Fig. 2 Thermogravimetric analysis of zeolites omega obtained with 1,3,5-trioxane (a) and 1,4-dioxane (b) as organic molecules. Gels with the composition $10SiO_2$ – $1Al_2O_3$ – $2.2Na_2O$ – 7.5 R – 140 H_2O (where R is trioxane or dioxane) were crystallized at 115°C for 7 days under dynamic conditions.

Fig. 3 Evolution of XRD patterns of zeolites obtained from the crystallization of gels with the composition $10SiO_2$ – $0.82Al_2O_3$ – xNa_2O – 7.5 trioxane – 140 H_2O ($1.7 < x < 2.5$) at 115°C for 7 days under dynamic conditions. The pattern of a pure mordenite is added for comparison. The arrow in pattern (f) indicates the position of the (016) reflection of the **EON** topology. Red triangles in pattern (f) point out the position of XRD peaks characteristic of the **EON** structure that are not present in **MAZ** and whose intensity increases with the Na_2O content in the gel.

Fig. 4 SEM pictures of zeolites obtained from the crystallization of gels with the composition $10SiO_2$ – $0.82Al_2O_3$ – xNa_2O – 7.5 trioxane – 140 H_2O at 115°C for 7 days under dynamic conditions. (a) and (b): zeolite omega ($x = 2.5$); (c) and (d) ECR-1 ($x = 1.7$).

Fig. 5 ^{27}Al NMR spectra of zeolites obtained from the crystallization of gels with the composition $10SiO_2 – 0.82Al_2O_3 – xNa_2O – 7.5$ trioxane – 140 H_2O ($1.7 < x < 2.5$) at 115°C for 7 days under dynamic conditions. The inset shows an example of deconvolution of the signal using two symmetric lines.

Fig. 6 XRD pattern (a) and SEM pictures (b, c) of zeolite ECR-1 obtained from the crystallization of a gel with the composition $10SiO_2 – 0.82Al_2O_3 – 1.7Na_2O –$ 7.5 trioxane – 140 H_2O at 130°C for 7 days under dynamic conditions.

Fig. 7 XRD pattern (a) and SEM pictures (b, c) of zeolite omega obtained from the crystallization of a gel with the composition $10SiO_2 – 1Al_2O_3 – 2.2Na_2O –$ 7.5 dioxane – 140 H_2O at 115°C for 7 days under dynamic conditions.

Fig. 8 XRD patterns of zeolites obtained from the crystallization of a gel with the composition $10SiO_2 – 1Al_2O_3 – xNa_2O –$ 7.5 dioxane – 140 H_2O for 7 days under dynamic conditions. x = 2.2, T = 115°C (a); x = 1.7, T = 115°C (b); x = 1.7, T = 130°C (c). Black triangles and dashed lines in (c) point out the position of peaks characteristic of **MOR** that are not present in **MAZ**.

Fig. 9 ^{23}Na MAS NMR spectra of zeolites ECR-1 and omega in the dehydrated and rehydrated phases.

Fig. 10 ^{23}Na NMR spectra of calcined rehydrated zeolites obtained from the crystallization of gels with the composition $10SiO_2 – 0.82Al_2O_3 – xNa_2O –$ 7.5 trioxane – 140 H_2O ($1.8 < x < 2.5$) at 115°C for 7 days under dynamic conditions. The inset shows an example of deconvolution of the signal using signals of pure zeolite omega (blue) and pure ECR-1 (black).

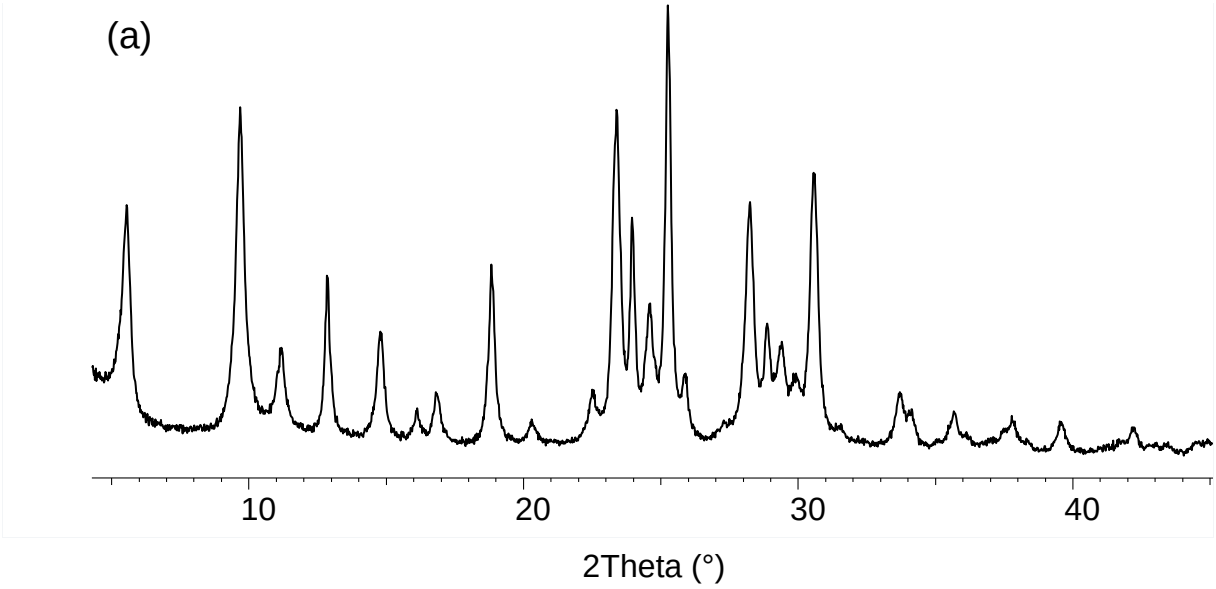

(b)

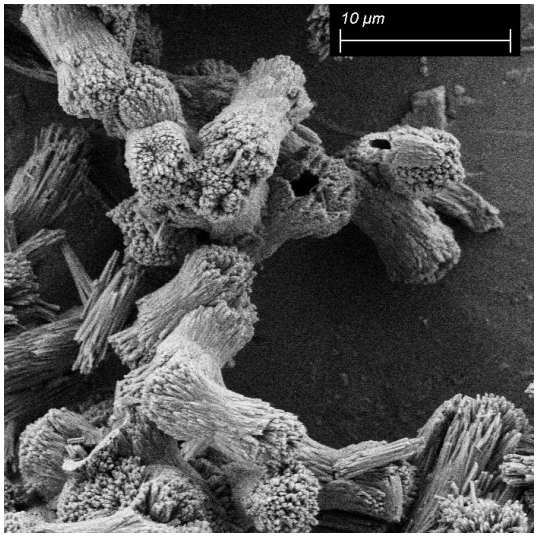

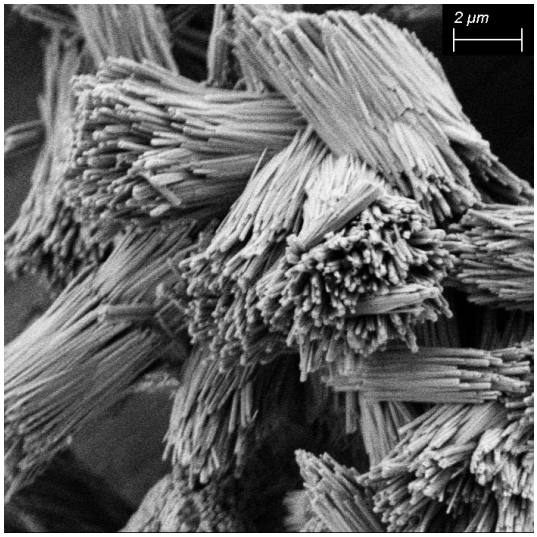

Figure 1

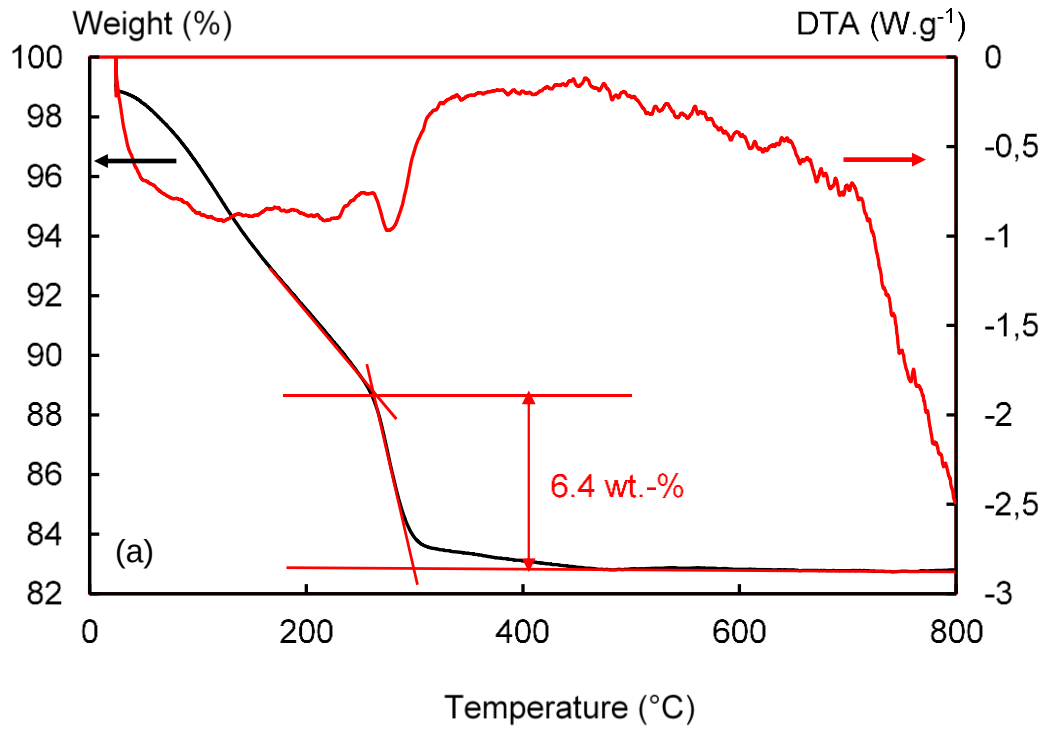
Weight (%)
DTA (W.g-1)
100
98
96
94
92
90
88
86
84
82
0
-0,5
-1
-1,5
-2
-2,5
-3
6.4 wt.-%
(a)
0
200
400
600
800
Temperature (°C)

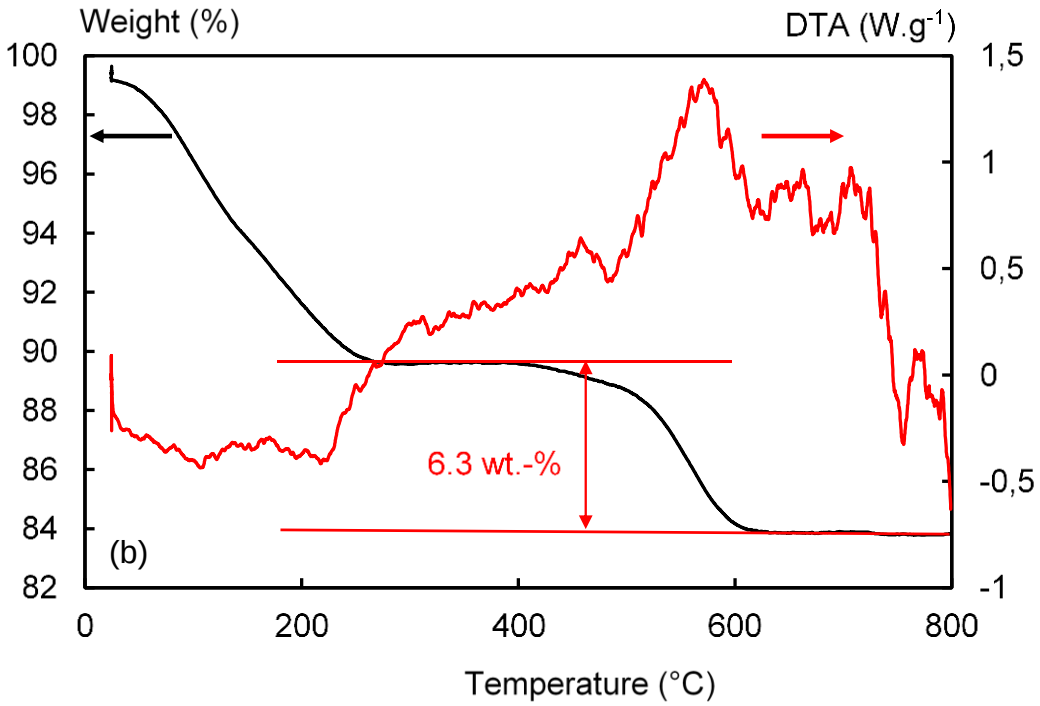
Weight (%)
DTA (W.g-1)
100
98
96
94
92
90
88
86
84
82
1,5
1
0,5
0
-0,5
-1
6.3 wt.-%
(b)
0
200
400
600
800
Temperature (°C)

Figure 2

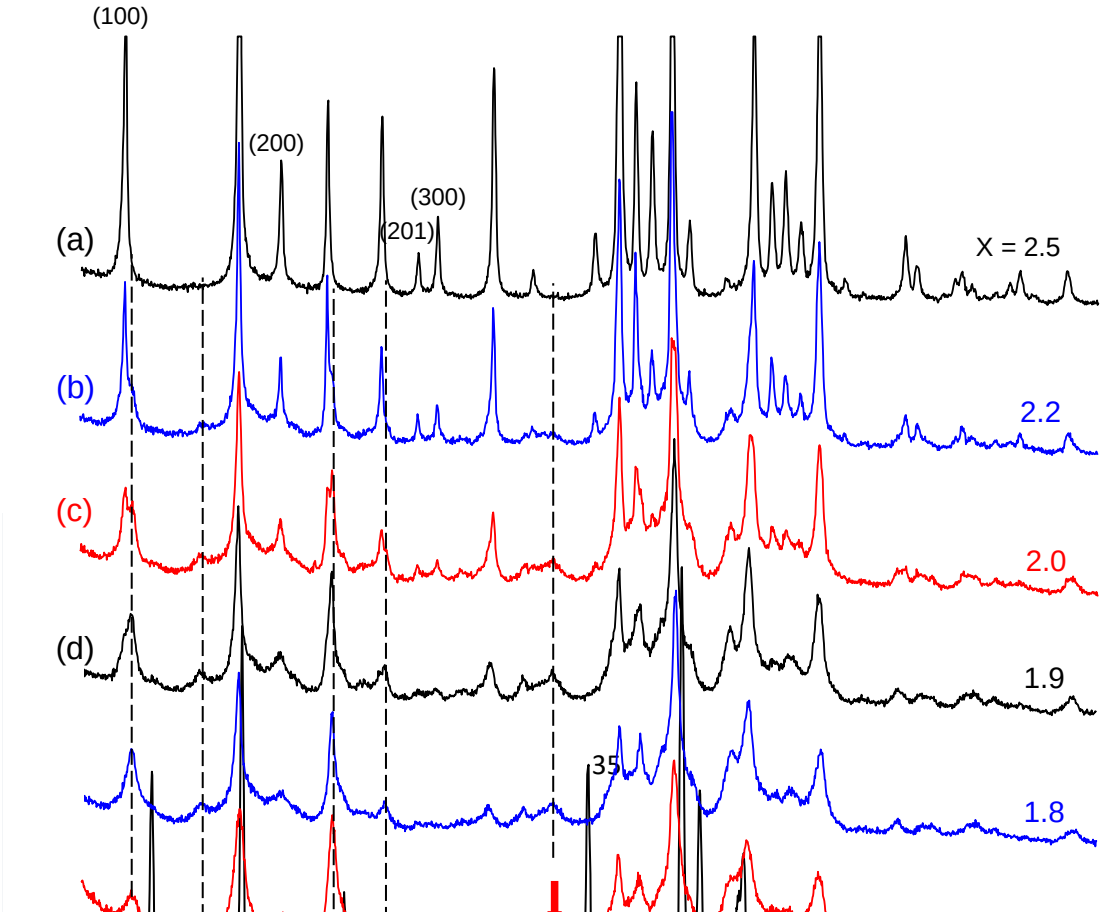
(100)
(200)
(300)
(201)
(a)
X = 2.5
(b)
2.2
(c)
2.0
(d)
1.9
35
1.8

(e)

(f) (016)

▲ ▲ ▲

Figure 3

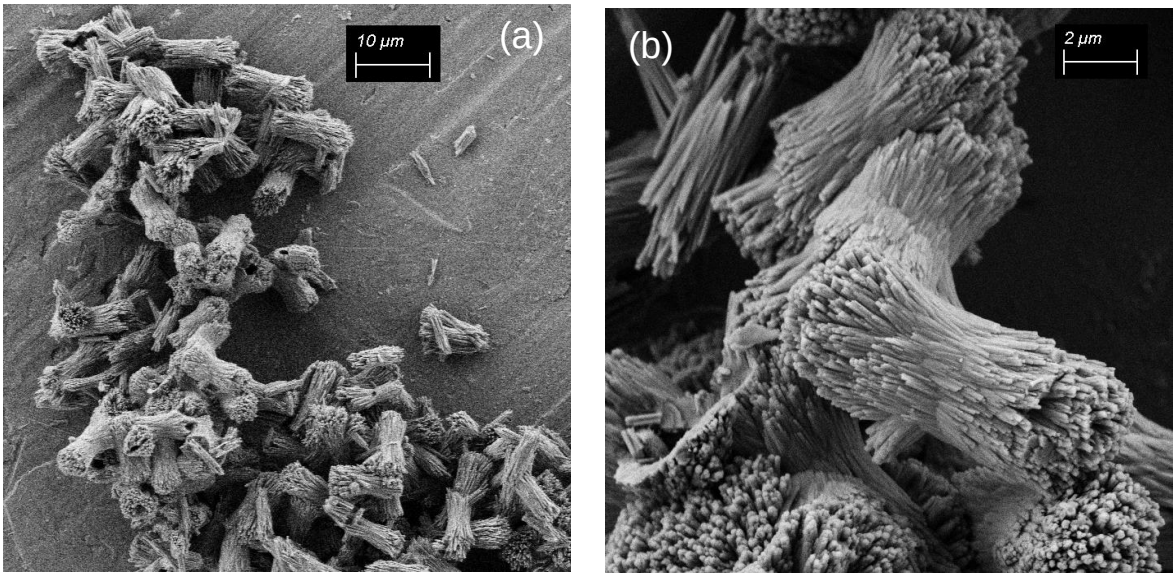

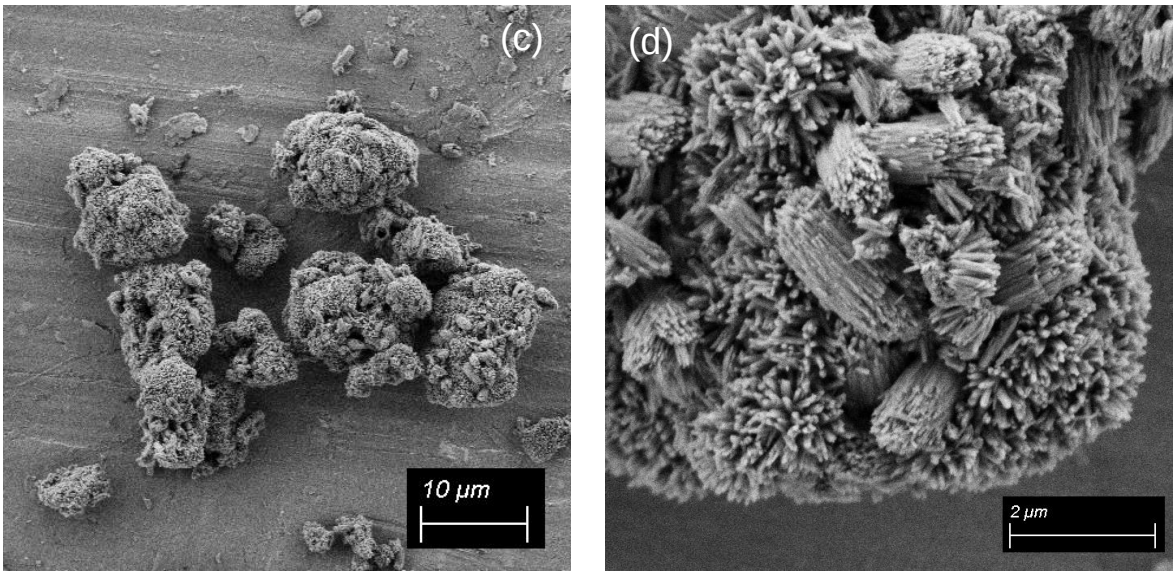

Figure 4

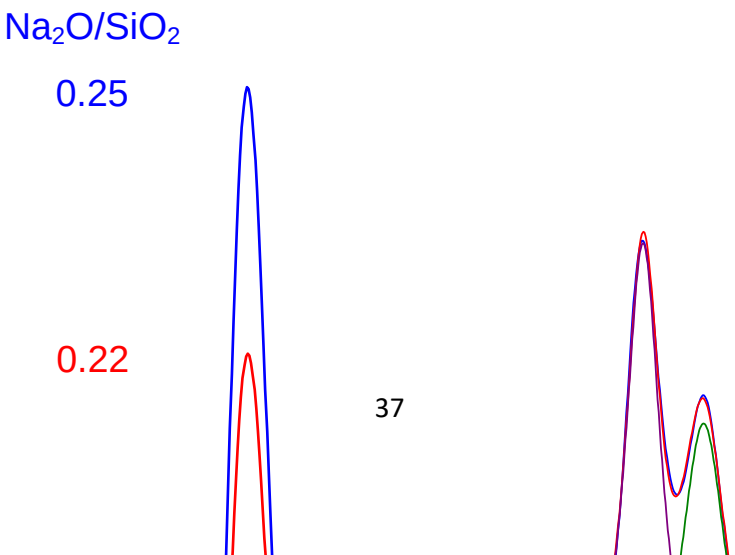

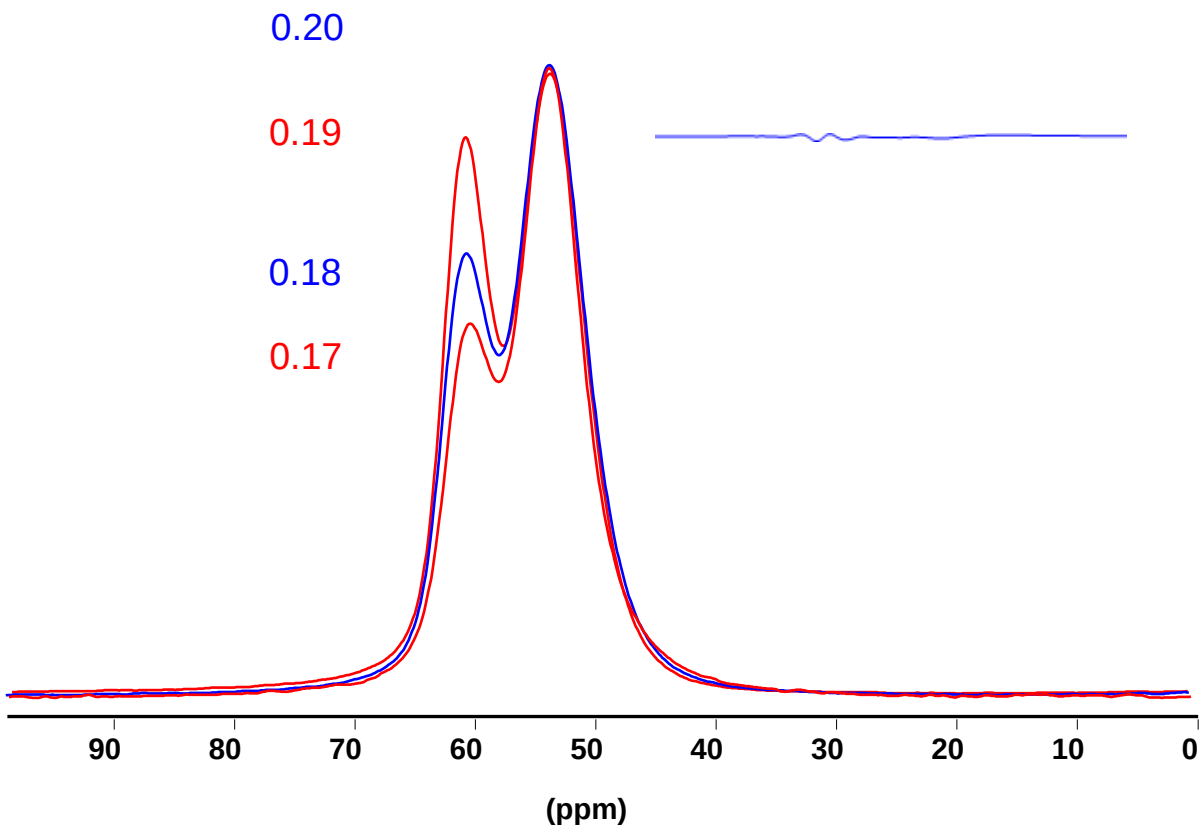

Figure 5

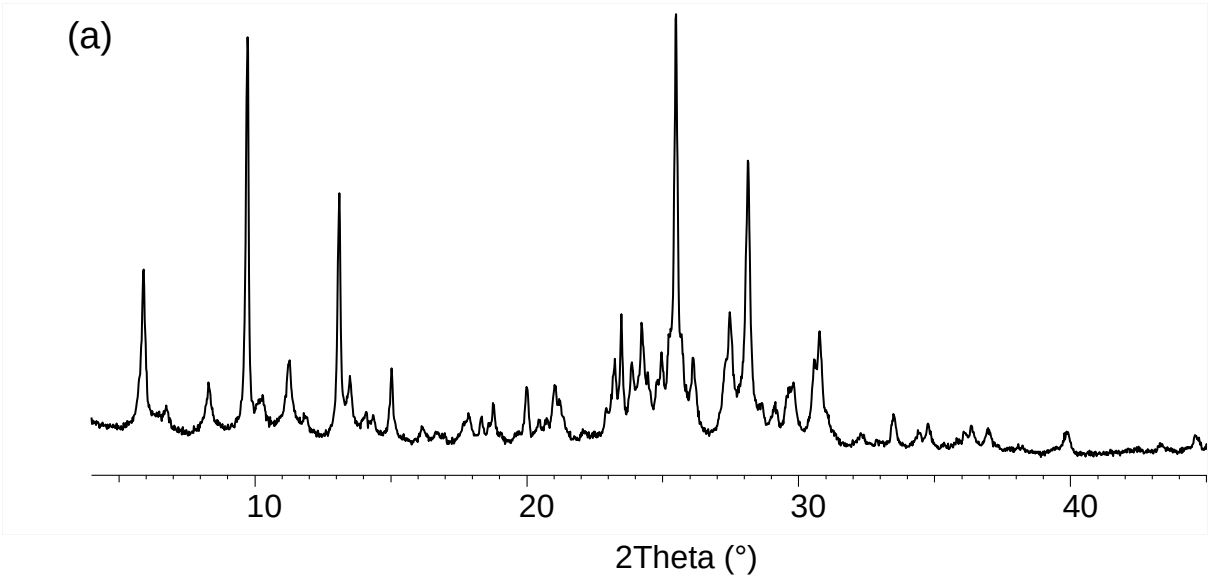

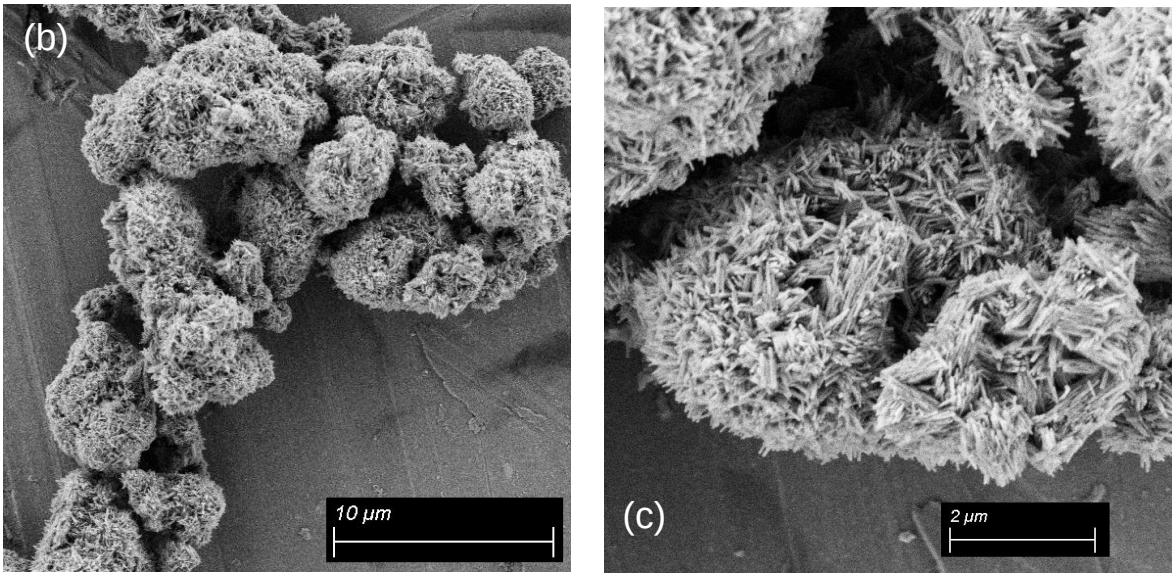

Figure 6

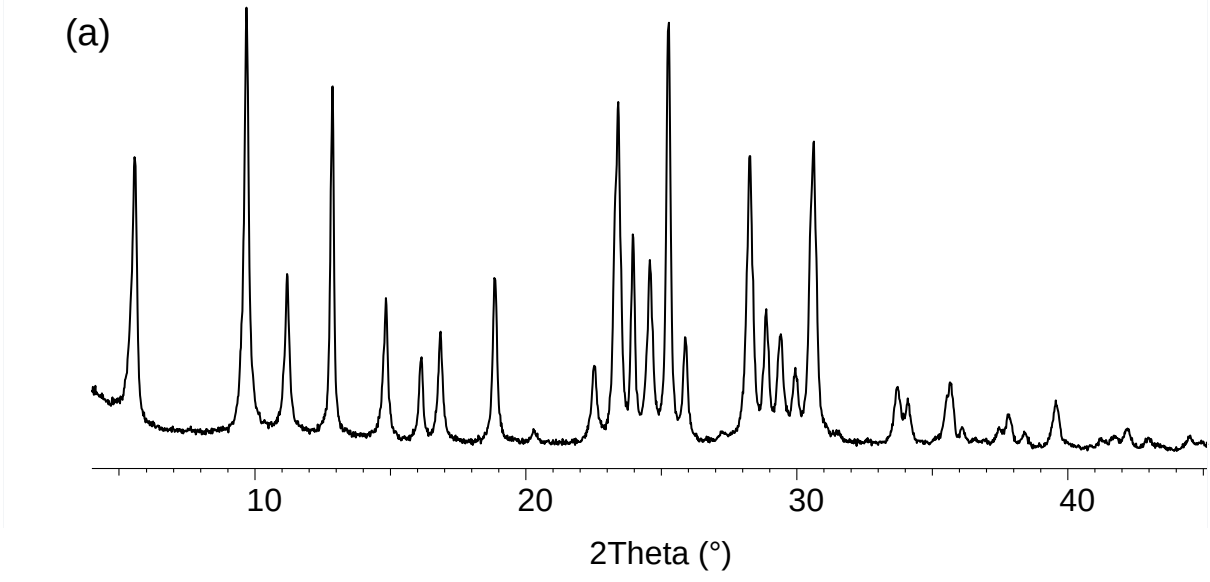

▲

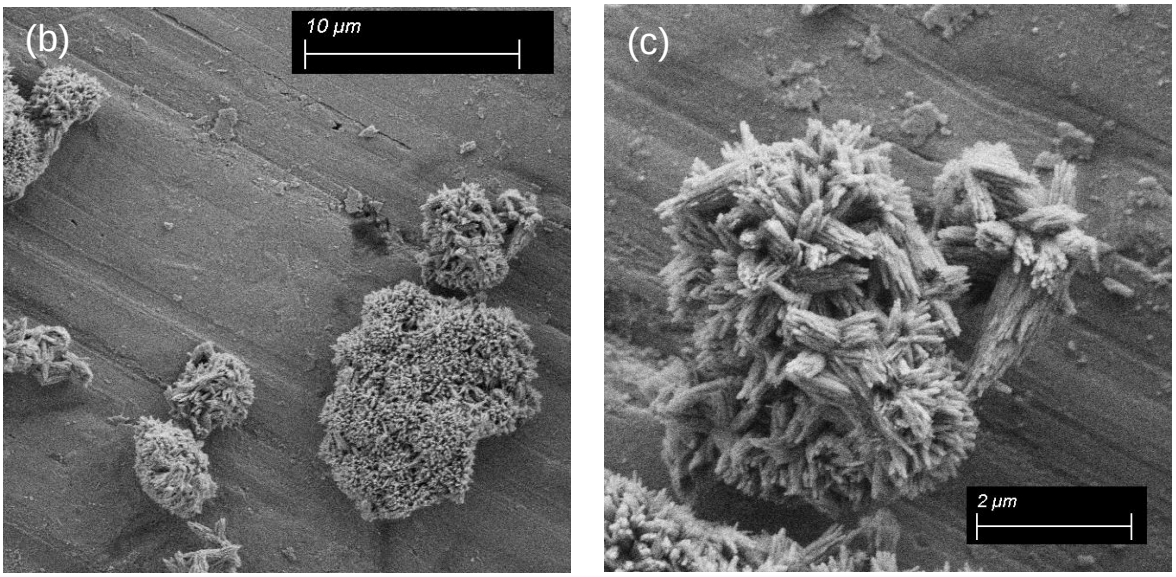

Figure 7

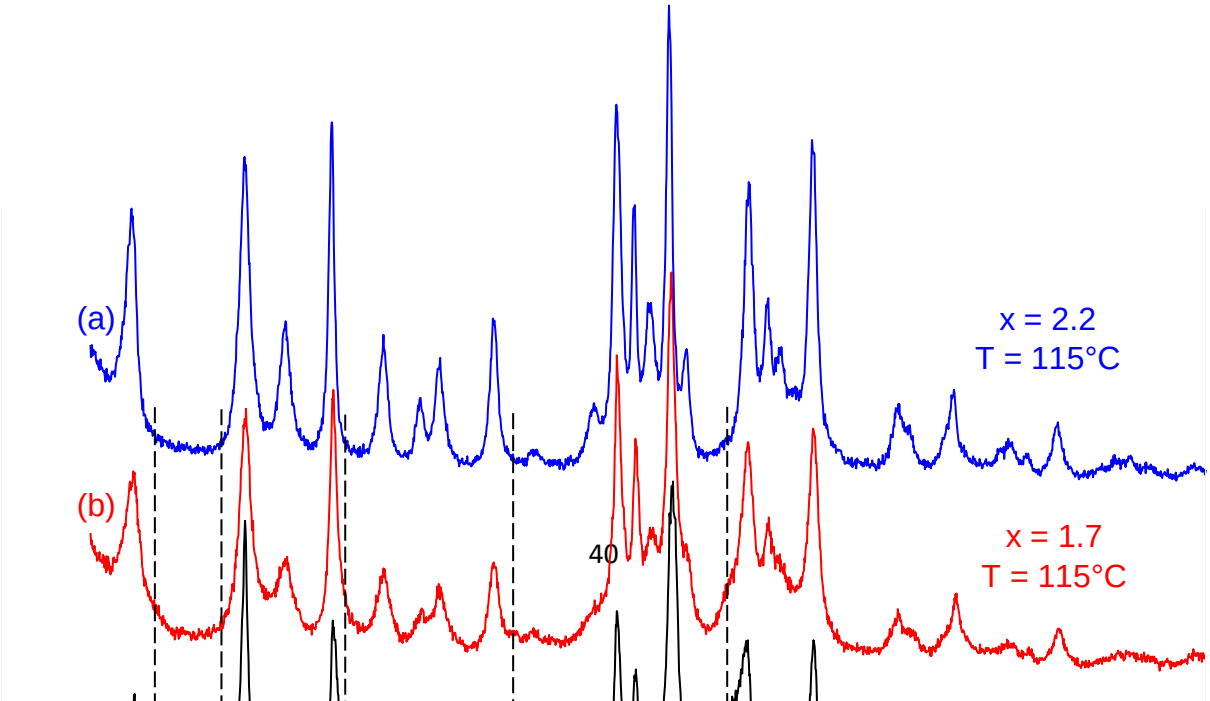

(c)

▲

Figure 8

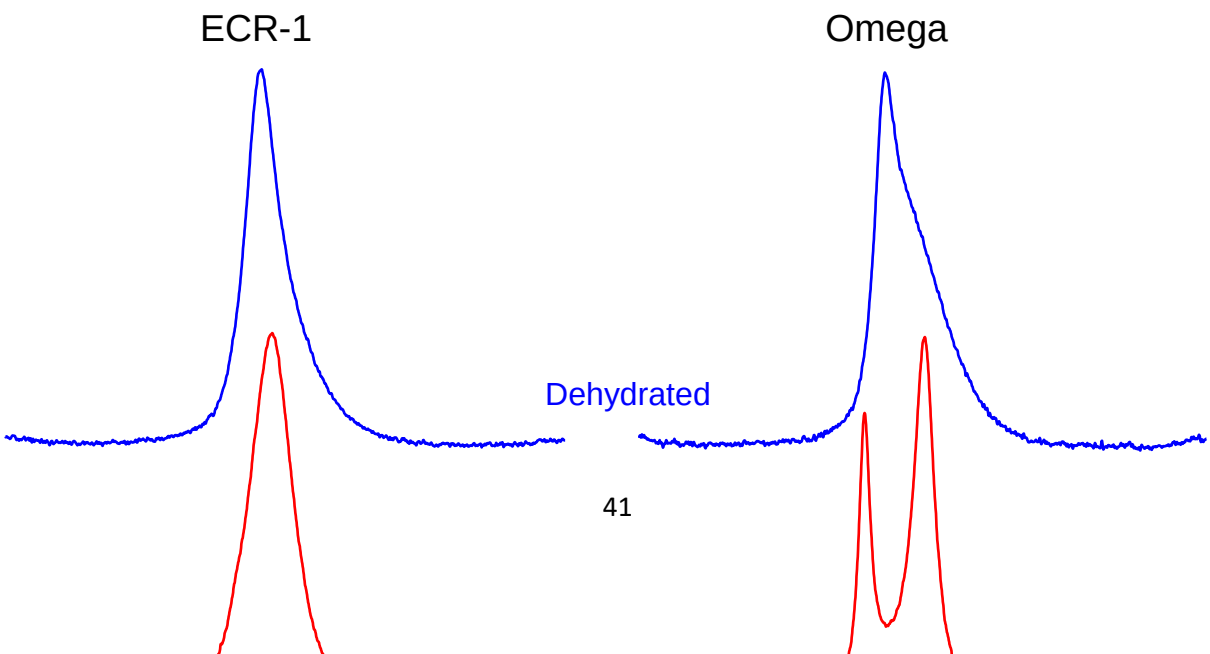

Rehydrated

Figure 9

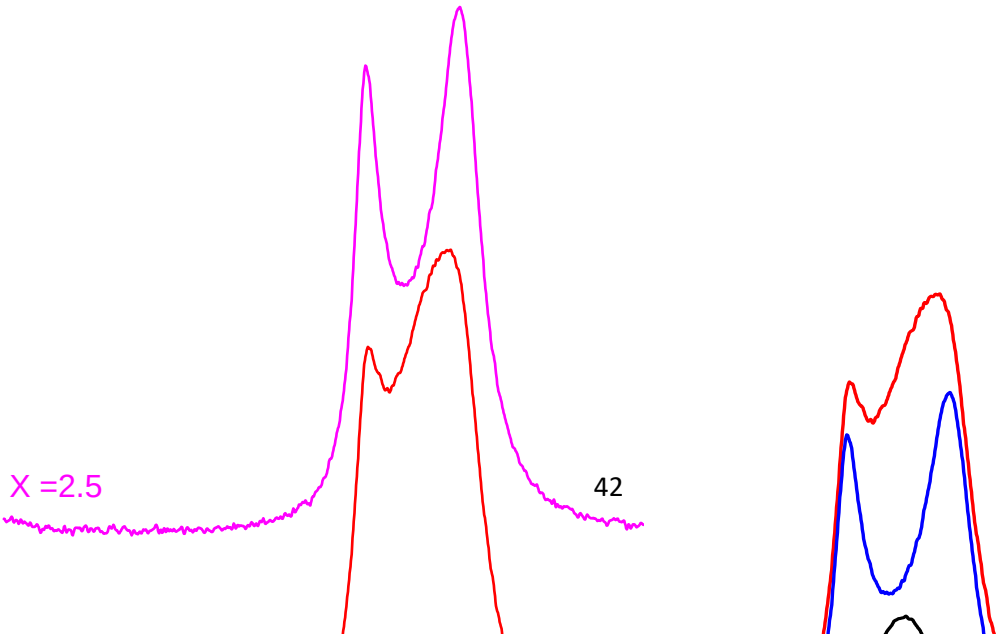

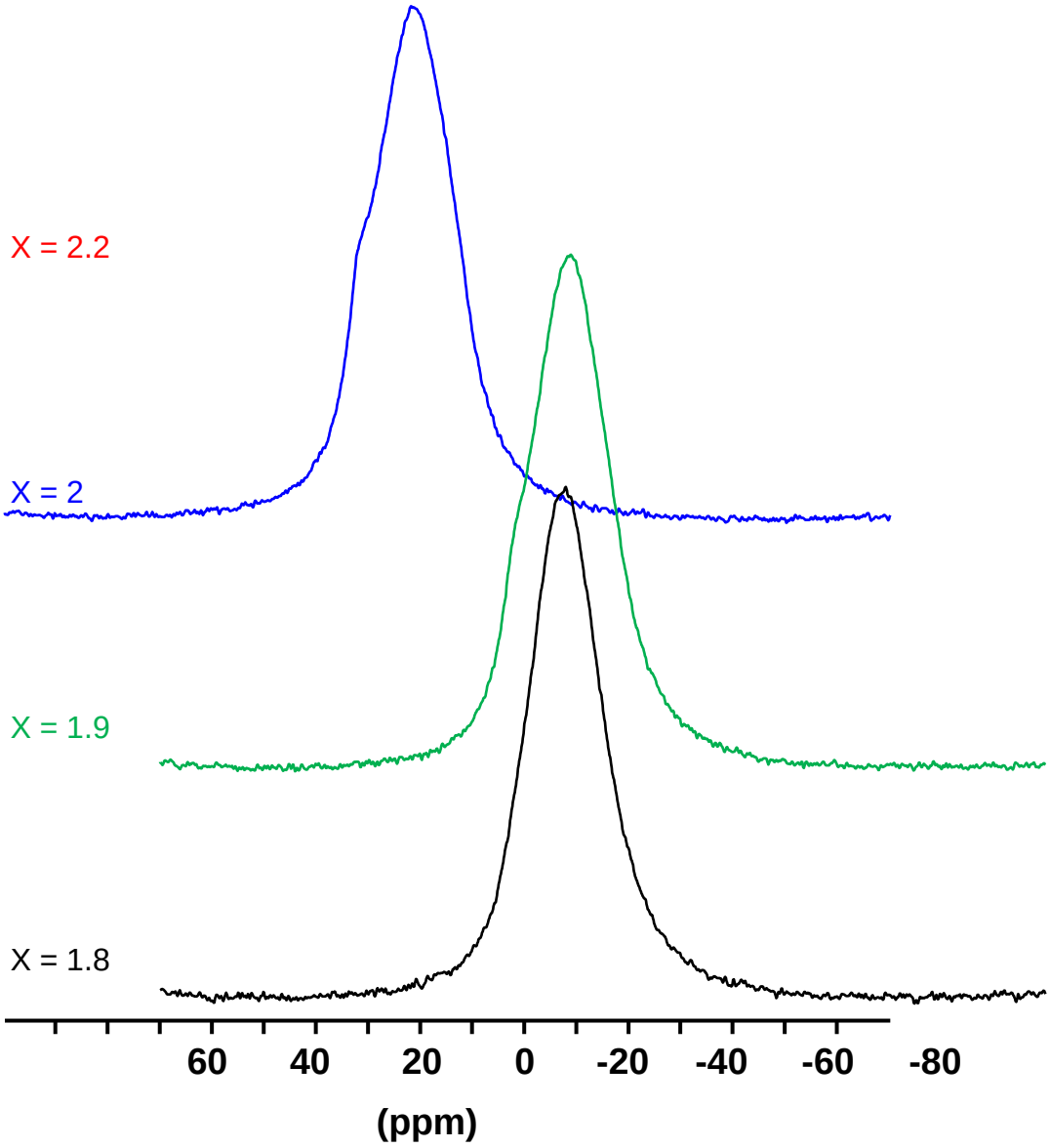

Figure 10